Papillomavirus Research 7 (2019) 88–96

Contents lists available at ScienceDirect

Papillomavirus Research

journal homepage: www.elsevier.com/locate/pvr

Viral genome integration of canine papillomavirus 16

Jennifer Luff[a,*], Michelle Mader[a], Peter Rowland[b], Monica Britton[c], Joseph Fass[c], Hang Yuan[d]

[a] Department of Population Health and Pathobiology, North Carolina State University, Raleigh, North Carolina, USA
[b] Histopath Consulting, Worcester, MA, USA
[c] UC Davis Genome Center—Bioinformatics Core, University of California, Davis, CA, USA
[d] Department of Pathology, Georgetown University Medical Center, Washington, DC, USA

ARTICLE INFO

Keywords:
Canine
Papillomavirus
Squamous cell carcinoma
Integration
Carcinogenesis

ABSTRACT

Papillomaviruses infect humans and animals, most often causing benign proliferations on skin or mucosal surfaces. Rarely, these infections persist and progress to cancer. In humans, this transformation most often occurs with high-risk papillomaviruses, where viral integration is a critical event in carcinogenesis. The first aim of this study was to sequence the viral genome of canine papillomavirus (CPV) 16 from a pigmented viral plaque that progressed to metastatic squamous cell carcinoma in a dog. The second aim was to characterize multiple viral genomic deletions and translocations as well as host integration sites. The full viral genome was identified using a combination of PCR and high throughput sequencing. CPV16 is most closely related to chipapillomaviruses CPV4, CPV9, and CPV12 and we propose CPV16 be classified as a chipapillomavirus. Assembly of the full viral genome enabled identification of deletion of portions of the E1 and E2/E4 genes and two viral translocations within the squamous cell carcinoma. Genome walking was performed which identified four sites of viral integration into the host genome. This is the first description of integration of a canine papillomavirus into the host genome, raising the possibility that CPV16 may be a potential canine high-risk papillomavirus type.

1. Introduction

Papillomaviruses are circular double-stranded DNA viruses approximately 8 kb in length that are present in humans and many animal species [1,2]. These viruses are host and site specific [1,2]. They infect keratinocytes at either mucosal or cutaneous sites and most often cause benign proliferations, such as papillomas or plaques [1,2]. Typically, these lesions regress, although rarely they can persist and progress to cancer [2–4]. Human mucosal papillomaviruses are known to cause essentially all cases of cervical cancer [4]. They are divided into the low-risk and high-risk types, with the high-risk types associated with a higher risk of cancer development [2]. With human high-risk mucosal papillomaviruses, such as human papillomavirus (HPV) 16 and 18, viral integration into the host genome is a critical event in carcinogenesis, although the underlying mechanism is not entirely clear [3,5]. Unlike human mucosal high-risk papillomaviruses with a well-established causal association with cancer, human cutaneous papillomaviruses are only rarely associated with cancer. When this does occur, it is most often in patients with specific immunodeficiencies and many times in association with ultraviolet light exposure [6]. Integration of the viral genome has not been demonstrated for these cutaneous HPVs.

There are currently twenty-three canine papillomaviruses (CPVs), which comprise three different genera [7–21]. The largest group is the chipapillomaviruses, which are associated with pigmented viral plaques, followed by the taupapillomaviruses and the lambdapapillomaviruses [22]. Rarely have any canine papillomaviruses been associated with cancer development. The taupapillomavirus CPV2 has been associated with metastatic cutaneous squamous cell carcinoma in a research colony of dogs with X-linked severe combined immunodeficiency [23]. Apart from CPV2, there have been only rare, often individual reports of cancer associated with other canine papillomavirus types [13,24–27]. Never has there been demonstration of integration into the host genome.

The aims of this present study were to sequence the viral genome of canine papillomavirus (CPV) 16 and to characterize viral genomic translocations, deletions, and integration sites into the host genome. The clinical features of this case have been described previously and were presented alongside its biological male offspring [24]. Both dogs developed metastatic squamous cell carcinoma in association with a canine papillomavirus. The male offspring developed cancer in association with CPV12 and the dog in the present case with CPV16 [24]. The CPV16 genome has also been described previously in a genome announcement based upon this case [13].

* Correspondence to: 1060 William Moore Drive, Raleigh, NC 27612, USA.
E-mail address: jaluff@ncsu.edu (J. Luff).

https://doi.org/10.1016/j.pvr.2019.02.002
Received 31 October 2018; Received in revised form 30 January 2019; Accepted 12 February 2019
Available online 13 February 2019

2. Material and methods

2.1. Sample collection, histopathology, and diagnosis

Routine surgical biopsies were obtained from a 13 year-old Basenji dog that developed multiple cutaneous pigmented viral plaques, characterized histologically by epithelial hyperplasia and hyperkeratosis (Supplemental Figure 1 A) (clinical and pathological data presented in Luff et al., 2016) [24]. Within one plaque there was progression to invasive squamous cell carcinoma (SCC) (Supplemental Figure 1B). Additional surgical biopsies were obtained one year later at the site of the previously diagnosed squamous cell carcinoma as well as an enlarged draining lymph node. Biopsies confirmed regrowth of the squamous cell carcinoma as well as metastasis to the draining lymph node (Supplemental Figure 1 C). A fresh sample of the squamous cell carcinoma was saved frozen and stored at −80 °C. Histologic evaluation of the samples was performed by two board-certified veterinary pathologists (PR and JL).

2.2. Whole genome sequencing

2.2.1. Initial papillomavirus PCR

Genomic DNA was extracted from two 25 μm scrolls cut from the formalin fixed paraffin embedded (FFPE) tissue samples using a commercially available kit following manufacturer's recommended protocol (DNeasy tissue kit, Qiagen Inc., Valencia, CA). PCR was performed using a degenerate consensus primer set, CanPV/ FAP64 that has previously been used to identify multiple canine papillomavirus types [28]. PCR was performed using 100 ng of extracted DNA as previously described [28]. Additional sets of degenerate consensus primers (CPV sets 1–5, Supplemental Table 1) were designed using Primer3 design software (http://primer3.sourceforge.net). These primer sets were designed based upon conserved regions of canine papillomavirus genomes identified using nucleotide alignments of the following CPVs with their corresponding GenBank accession numbers in parentheses: CPV3 (NC_008297), CPV4 (NC_010226), CPV5 (FJ492743), CPV9 (NC_016074), CPV10 (NC_016075), CPV11 (JF800658), CPV12 (JQ754321). These additional primers aimed to amplify sequences from the remaining papillomavirus genome. PCR reaction conditions are as follows. Samples of genomic DNA were diluted with distilled water to yield a concentration of 10 ng/μl. The DNA sample (100 ng) was then amplified by PCR in a reaction mixture containing 10 mM Tris-HCl, 1.5 mM $MgCl_2$, 200uM each (800 μM) deoxynucleoside triphasphate (dNTP), 1 unit (0.2 μl) Taq polymerase (HotStar Taq DNA polymerase, Qiagen, Valencia, CA), and approximately 2 μM of each primer for a total reaction volume of 50 μl. All PCR reactions were performed on an Applied Biosystems GeneAmp PCR system 2700 thermocycler (Foster City, CA). An initial activation step of 95 °C for 10 min was followed by 50 cycles of 1) 1 min denaturation at 95 °C 2) 1 min annealing at 50 °C, and 3) 2 min elongation at 72 °C. There was a hold for 7 min at 72 °C and a final hold at 4 °C.

All PCR products were electrophoresed through a 1% agarose gel and visualized with a DNA stain (GelRed, Phenix Research Products, Candler, NC). PCR products were cut from the gel and purified using a commercially available kit (Promega Wizard SV Gel and PCR Clean-Up System, Promega Corp., Madison, WI). Purified PCR products were submitted to a routine sequencing laboratory (Eton Bioscience, San Diego, CA) and the resulting nucleotide sequences were analyzed for sequence similarity to known papillomavirus types using the BLAST tool of the National Center for Biotechnology Information (NCBI).

2.2.2. High throughput sequencing

High throughput sequencing (HTS) using the Illumina, Hiseq. 2500 platform (UC Davis Genome Center, Davis, CA) was performed on extracted DNA (DNeasy Blood and Tissue Kit, Qiagen, Inc.) from the fresh frozen sample of squamous cell carcinoma. Raw reads were trimmed to remove the adaptor contamination and low-quality sequences using Scythe and Sickle (https://github.com/ucdavis-bioinformatics), and were aligned to the *Canis familiaris* genome using BWA's short read aligner [29]. Read pairs that aligned to the dog genome or to phiX were set aside. The remaining reads were run through the PRICE assembler seeded with two fragments (315 bp and 494 bp) of viral genome that were amplified and sequenced using degenerate primers above [30].

2.2.3. Overlapping PCR

Additional overlapping sets of primers (ConSet1–5, Supplemental Table 1) were designed using Primer3 design software and included specific primers designed from the HTS sequence (ConSet1 For and ConSet5 Rev) and new degenerate consensus primers designed based upon nucleotide alignments of the following CPVs with their corresponding GenBank accession numbers in parentheses: CPV3 (NC_008297), CPV4 (NC_010226), CPV5 (FJ492743), CPV9 (NC_016074), CPV10 (NC_016075), CPV11 (JF800658), CPV12 (JQ754321). PCR was performed as described above using 100 ng of extracted DNA from the FFPE pigmented viral plaque samples with the exception that only 45 cycles were used in the cycling conditions. One set of primers (ConSet #2) produced a product with a novel sequence 279 basepair (bp) in length. Two additional overlapping sets of specific primers (ChanaSet 7 and ChanaSet MM, Supplemental Table 1) were then generated using this new sequence fragment and the HTS sequence. PCR was performed as described above with the following changes: 1.5 mM $MgCl_2$ was reduced to 0.5 mM and only 100 uM each (400 μM) deoxynucleoside triphasphate (dNTP) were used; 45 cycles were run with an annealing temperature of 57 °C.

Additional PCR and nucleotide sequencing was performed using multiple sets of specific primers for CPV16 using DNA extracted from FFPE pigmented plaques and the fresh SCC sample. These primer sets (listed Supplemental Table 2) included ChanaSet 7 (above), ChanaSet 9, and ChanaSet 11. PCR was performed as described above for ChanaSet 7 with the exception that only 50 μM each (20 μM) deoxynucleoside triphasphate (dNTP) were used and only 40 cycles were run at an annealing temperature of 58 °C. PCR using the primer set ChanaSet 14 (Supplemental Table 2) was run using genomic DNA extracted from the fresh SCC sample and viral plaque sample and reaction conditions as stated above for ChanaSet 9 with the exception that $MgCl_2$ was not added and 45 cycles were run.

All PCR products were electrophoresed through a 1% agarose gel, purified, and sequenced as described above. The resulting nucleotide sequences were analyzed using BLAST. Vector NTI Advance 10 sequence analysis software (Invitrogen, Carlsbad, CA) was used to assemble the sequence contigs containing high-quality trace files.

2.3. Genomic organization and phylogenetic analysis

Putative open reading frames (ORFs) and their corresponding amino acid sequence were predicted using Vector NTI Advance 10 sequence analysis software (Invitrogen). A phylogenetic tree was generated from an alignment of the L1 nucleotide sequences using the neighbor-joining method with commercially available software (CLC Sequence Viewer 7, Germantown, MD). The following CPVs with their corresponding GenBank accession numbers were used in the analysis: CPV1 (D55633), CPV2 (NC_006564), CPV3 (NC_008297), CPV4 (NC_010226), CPV5 (FJ492743), CPV6 (NC_013237), CPV7 (FJ492742), CPV8 (NC_016014), CPV9 (NC_016074), CPV10 (NC_016075), CPV11 (JF800658), CPV12 (JQ754321), CPV13 (NC_023852), CPV14 (NC_019852), CPV15 (JX899359), CPV17 (KT272399), CPV18 (KT326919), CPV19 (KX599536). The predicted E6 and E7 protein sequences for CPV16 were aligned with the E6 and E7 protein sequences for CPV2 (NC_006564), CPV10 (NC_016075), CPV12 (JQ754321), HPV4 (NC_001457), HPV5 (NC_001531), HPV9 (NC_001596), HPV16 (NC_001526), HPV18 (NC_001357), and HPV95 (AJ620210) using Vector NTI Advance 10 sequence analysis software.

2.4. Genome walking

Genome walking was performed using the Universal GenomeWalker kit (Clontech Laboratories, Mountain View, CA) following manufacturer's recommended protocols. Initially, the fresh SCC tissue sample was processed using the NucleoSpin Tissue Genomic DNA purification kit according to the manual. The isolated DNA was then digested overnight at 37 °C with the restriction enzymes DraI, *Eco*RV, *Pvu*II, and StuI in separate reactions. The digestion reactions were then purified using the Nucleospin gel and PCR clean up kit, following the protocol in genome walker manual. The genome walker adaptors were then ligated to the digested libraries in a reaction mixture containing 4.8 µl digested purified DNA, 1.9 µl genome walker adaptor, 0.8 µl 10X ligation buffer, and 0.5 µl T4 DNA ligase. The mixture was incubated overnight at 16 °C followed by 5 min at 70 °C to stop the reaction. A PCR reaction was then performed using the adaptor primer and gene specific primers (Supplemental Table 3). Omission of the DNA template served as a negative control. The positive control library provided in the kit with the associated primer served as a positive control. The PCR reaction contained 19.5 µl water, 2.5 µl 10X Advantage 2 PCR buffer, 0.5 µl dNTP (10 mM each), 0.5 µl each primer (10 µM), 0.5 µl Advantage 2 polymerase mix, and 1 µl of each DNA library. PCR reactions were performed on an Applied Biosystems GeneAmp PCR system 2700 thermocycler. An initial 7 cycles of 1) 94 °C for 25 s 2) 72 °C for 3 min were followed by 32 cycles of 1) 94 °C for 25 s 2) 67 °C for 3 min, with a final 7 min at 67 °C. Secondary PCR was performed using 1 µl of the PCR reaction diluted in 49 µl water with the adaptor primer 2 and a gene specific primer in the combinations listed in Supplemental Table 3. The secondary PCR reaction mixture was as described above for the primary PCR reaction. Secondary PCR reaction conditions included an initial 5 cycles of 1) 94 °C for 25 s 2) 72 °C for 3 min followed by 20 cycles of 1) 94 °C for 25 s 2) 67 °C for 3 min with a final 7 min at 67 °C.

All PCR products were electrophoresed through a 1% agarose gel and visualized with a DNA stain. PCR products were cut from the gel and purified using a commercially available kit (Promega Wizard SV Gel and PCR Clean-Up System). Purified PCR products were submitted to a routine sequencing laboratory (Eton BioSciences) as well as routinely cloned into the Topo-TA cloning kit (ThermoFisher Scientific, Waltham, MA) following their recommended protocols. Resulting clones were purified using a miniprep kit (QIAprep Spin Miniprep Kit, Qiagen, Germantown, MD) following manufacturer's recommended protocols and submitted for sequencing to a routine laboratory (Eton BioSciences). The resulting nucleotides sequences were analyzed using the BLAST tool of the National Center for Biotechnology Information (NCBI) and the *Canis familiaris* genome (CanFam 3.1).

2.5. Viral mRNA expression

Real time PCR was performed to measure the viral copies of CPVs and the expression level of viral mRNA using extracted total DNA and extracted total RNA from the FFPE tissue samples of the viral plaque (early lesion), SCC (late lesion), and the lymph node containing metastatic SCC (late lesion). Total DNA was extracted as described above, respectively. Total RNA was extracted using a commercially available kit following manufacturer's recommended protocol (E.Z.N.A. FFPE RNA kit, Omega, Norcross, GA) and cDNA synthesis carried out on 1000 ng of purified RNA using a commercially available kit (QuantiTect RT kit, Qiagen, Valencia, CA). The resulting 20 µl of cDNA was further diluted with 180 µl water. A standard curve was generated using a dilution series of purified PCR products for each primer set. Primer sets for CPV16 E7 and the reference gene RPL13A (GenBank accession number NM_001313766) (Supplemental Table 4) were designed using Primer3 design software. Primers for GAPDH, also listed in Supplemental Table 4, have been previously published [31]. Real time PCR was performed in a reaction mixture containing 12.5 µl of Sybr green (QuantiTect Sybr green PCR kit, Qiagen), 0.5 µl of each primer (diluted to 10 µM), 1.5 µl water, and either 10 µl (concentration 10 ng/µl) total DNA, 10 µl diluted cDNA, or 10 µl of diluted purified PCR product (standard curve) for a total reaction volume of 25 µl. Real time PCR was run on the Roche LightCycler 480 (Roche Molecular Systems, Inc., Brighton, MA). An initial activation step of 95 °C for 13.5 min was followed by 50 cycles of 1) 10 s denaturation at 95 °C and 2) 1 min annealing at 57 °C. A melt curve was performed at the conclusion of the reaction. Analysis was carried out using the Roche LightCycler 480 Software (Roche Molecular Systems, Inc.). Primer efficiency was calculated from the standard curves. All samples were run in duplicate and mean values calculated. The standard curves were used for absolute quantification of the DNA samples to determine copy number. CPV16 copy number was normalized to copies of the reference gene RPL13A. Relative CPV16 E7 mRNA expression was determine by first normalizing expression to the reference gene GAPDH and calibrating all samples to mean expression in the plaque sample ($2^{-\Delta\Delta Cq}$ method) [32].

3. Results

3.1. CPV genotyping

Genomic DNA was extracted from two formalin fixed paraffin blocks containing tissue from multiple pigmented viral plaques (labeled Plaques A and Plaques B), one block of lymph node with metastatic squamous cell carcinoma (labeled LN SCC), and one block of squamous cell carcinoma (labeled skinSCC). PCR was performed on the extracted DNA using degenerate consensus primers (CanPV/FAP64) known to amplify multiple canine papillomavirus types (Supplemental Figure 1D) [28]. Sequence analysis of the amplicon from Plaques A revealed an approximately 300 bp sequence that shared approximately 99% sequence nucleotide identity to CPV12. Sequence analysis of the amplicons from Plaques B, LN SCC, and skinSCC revealed a 315 bp sequence that shared less than 80% nucleotide identify to any known papillomavirus type. In an attempt to sequence the entire viral genome, both rolling circle amplification and inverse PCR using genomic DNA extracted from the fresh frozen sample of squamous cell carcinoma were performed but failed (data not shown). This suggested the possibility that the fresh sample of SCC did not contain the entire viral genome and conventional methods to sequence the viral genome would be unsuccessful. We therefore attempted to identify the full viral genome using tissue from the original biopsy of the viral plaques (Plaques B), which were more likely to contain the entire viral genome. These samples, however, were all formalin fixed and paraffin embedded, which limited our ability to amplify large fragments. We therefore attempted to identify the full viral genome by generating a series of overlapping short (< 500 bp) amplicons from the FFPE pigmented viral plaque sample. One of the consensus primer sets (CPV Set #2) generated a novel amplicon, which was 494 bp in length and shared less than 80% nucleotide identify to any known papillomavirus type.

3.2. Whole genome sequencing

High throughput sequencing (HTS) was then performed using extracted DNA from the fresh frozen sample of squamous cell carcinoma. 227 M 100 bp paired-end reads were generated. After trimming, 208M paired-end trimmed reads were aligned to the *Canis familiaris* and phiX genomes. 1.6 M paired-end reads that did not align to these genomes were considered candidate viral sequences and were used in the assembly process.

The two initial nucleotide fragments generated with the CanPV/FAP64 and CPV Set #2 primer pairs were used to seed PRICE assembler and a 6454 bp fragment of the viral genome was sequenced. To obtain the remaining sequence, we performed PCR using a combination of specific primers and consensus primers on the sample of viral plaques (Plaques B). After this round of PCR, a single fragment was identified

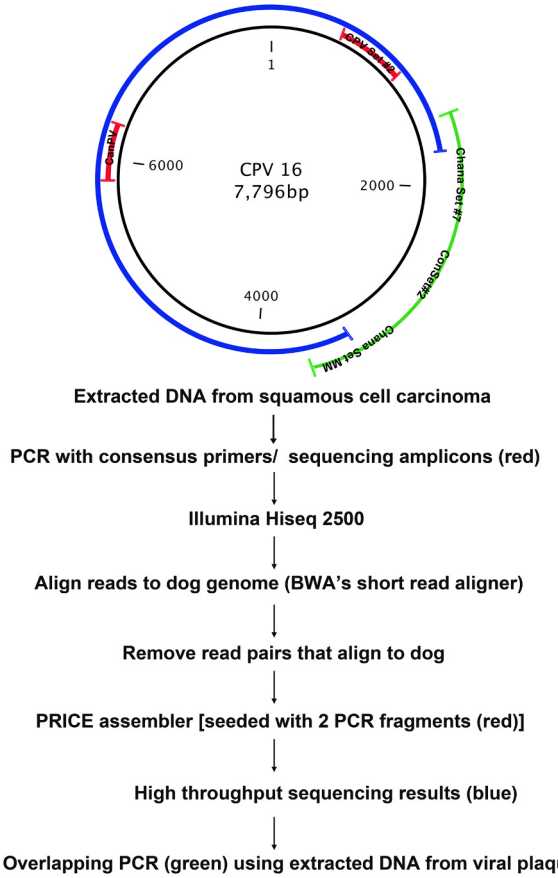

Fig. 1. Schematic representation of the sequencing methodology to generate full-length canine papillomavirus (CPV) 16 genomic sequence. Genomic DNA was extracted from a sample of squamous cell carcinoma and two segments of viral genome were identified using degenerate papillomavirus primers followed by amplicon sequencing (fragments indicated in red). Illumina Hiseq was then performed and all read pairs that aligned to dog were removed. PRICE assembler was then seeded with the two initial viral genome fragments (red), which enabled identification of a 6454 base pair sequence of the viral genome (indicated in blue). The remaining viral genome was identified using overlapping amplicons generated with combinations of specific and degenerate primers on DNA extracted from the original viral plaque (green).

using the ConSet#2 primers. Another round of PCR was then performed with specific primers designed within the new ConSet#2 fragment and specific primers designed within the larger fragment from HTS. This final round of PCR generated the final sequences that enabled assembly of the full viral genome. The sequencing methodology is outlined in Fig. 1.

3.3. Genomic organization and phylogenetic analysis

The full-length genomic sequence of CPV16 is deposited in GenBank, accession number NC_026640. The genome is 7796 base pairs in length with a typical genomic organization of papillomaviruses, and is predicted to contain a long control region (LCR), six early and two late genes (Fig. 2A). The predicted open reading frames include E6 (1–456), E7 (416–712), E1 (702–2594), E2 (2536–3957), E4 (3107–3718) and E5 (3978–4124), L2 (4148–5653) and L1 (5565–7202) (shown in Fig. 2A). Classification of papillomavirus types is based upon nucleotide alignments of the L1 ORF, which is the most conserved PV gene [1,33,34]. Alignment of the nucleotide sequences of the L1 genes to the other known canine PV types revealed that CPV4 (72% identity), CPV9 (72% identity) and CPV12 (71% identity) were the closest related PVs. Fig. 2B shows the phylogenetic tree generated

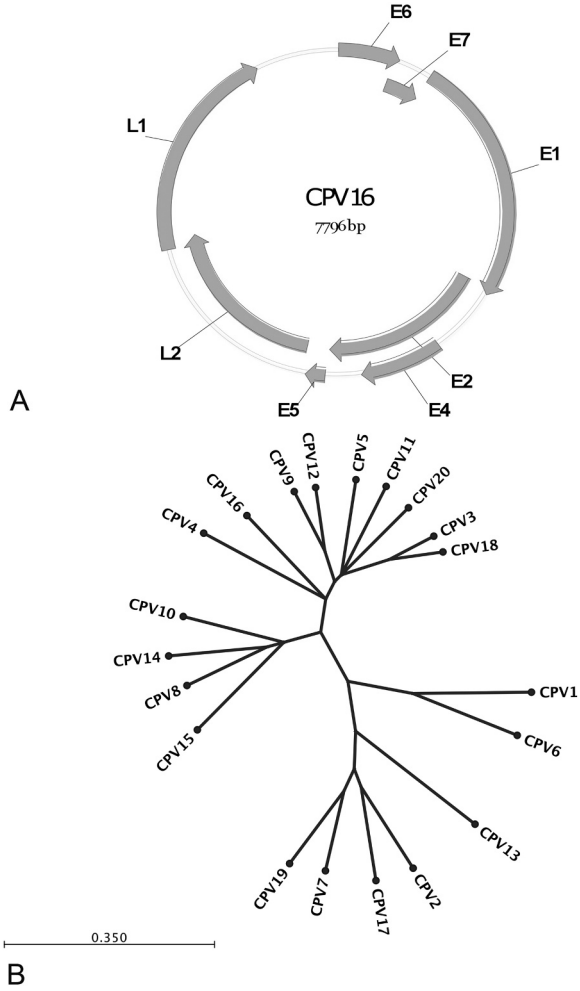

Fig. 2. (A) Schematic representation of circularized CPV16 genome and the organization of the open reading frames. (B) Phylogenetic tree of twenty canine papillomaviruses. The tree is based upon alignment of the L1 gene nucleotide sequences.

based upon this alignment of the L1 genes.

A protein alignment of CPV16 E6 to other E6 proteins from canine PVs (CPV10, CPV12, CPV2), human high risk mucosal PVs (HPV16 and HPV18), and human cutaneous PVs (HPV4, HPV5, HPV9, and HPV95) revealed two pairs of zinc binding CXXC motifs, which are common to most E6 proteins (Fig. 3A) [35]. The protein alignment of CPV16 E7 to other E7 proteins demonstrates the presence of the LXCXE peptide-binding motif similar to CPV10, CPV12, HPV16, and HPV5 [36–38]. This is in contrast to the alternate peptide-binding motif LXSXE present in CPV2, HPV4, and HPV95 (Fig. 3B) [39].

3.4. Viral gene translocations and deletions

High throughput sequencing identified only a portion of the viral genome, extending from 3295 to 1784 of CPV16, with no viral sequences identified between 1785 and 3294 (Fig. 4). There was a very uneven depth of coverage and no reads to indicate a circular genome (Fig. 4). Additionally, there was an 83 bp translocation from CPV16 LCR (7479–7562) to the terminal end of the HTS assembly located in the CPV16 E2/E4 genes (3295). At the opposite terminal end of the HTS assembly located in the CPV16 E1 gene (1278), there was an 85 bp translocation of the CPV16 E1 gene (1278–1363). Thus, the HTS assembly included the following nucleotide arrangement based upon the full CPV16 genome: 7479–7562:3295-(7796/1)-1784:1278–1363 (Fig. 4).

Fig. 3. (A) Protein alignment of E6 of multiple canine papillomaviruses (CPV) and human papillomaviruses (HPV). These viruses all share the conserved pairs of zinc binding CXXC motifs (indicated with horizontal bar). (B) Protein alignment of E7 of multiple CPVs and HPVs. CPV16 shares the LXCXE peptide-binding motif similar to CPVs 10 and 12 and HPVs 16 and 5. CPV2 and HPVs 4 and 95 contain the alternate peptide-binding motif LXSXE. HPV16 and HPV18 are human high-risk mucosal papillomaviruses and HPVs 4, 5, 9 and 95 are human cutaneous papillomaviruses. CPVs 2, 10, 12, and 16 are canine cutaneous papillomaviruses.

To verify that a portion of the CPV16 viral genome was deleted in the SCC sample, we performed conventional PCR for a region of the E1 gene, a region spanning E1 and E2, and a region spanning the LCR and E6. The sample of viral plaques revealed amplicons present for all 3 gene segments, whereas the sample of SCC contained an amplicon only using primers that amplified the LCR/E6 gene. No amplicons were generated with the E1 or E1/E2 primer sets (Fig. 5A).

During sequencing, one primer set (Chana Set #14) that amplified a

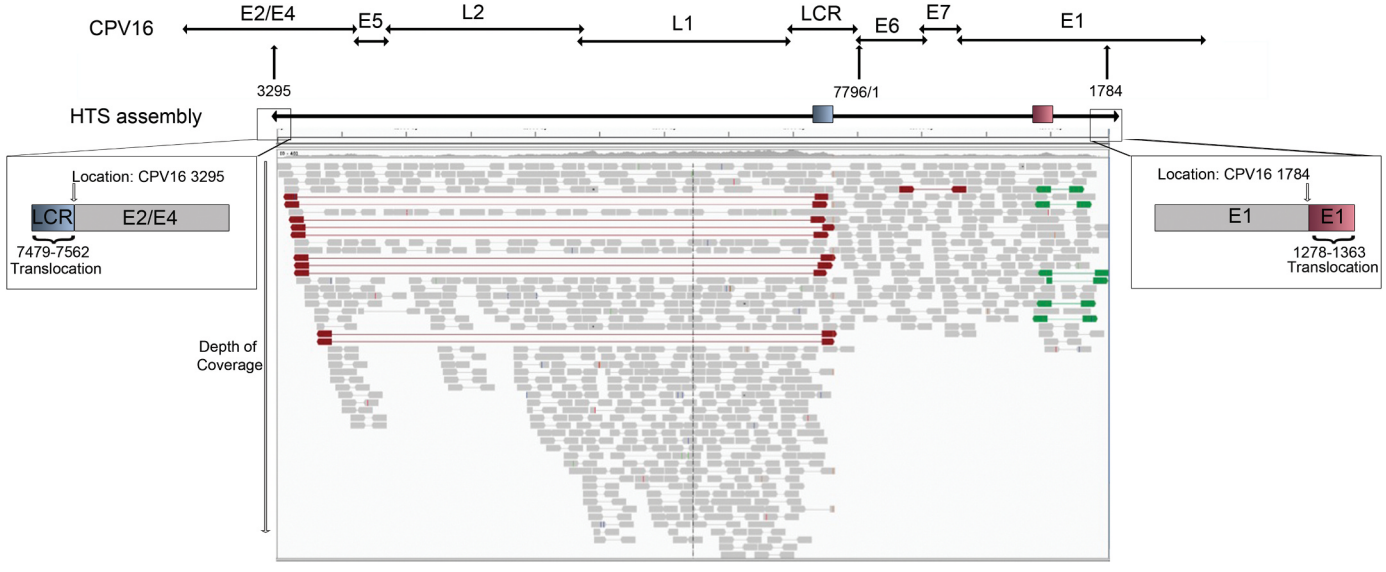

Fig. 4. Schematic depiction of the results of high throughput sequencing (HTS), including location of two translocations at both ends of the assembly. The results of HTS identified a 6454 basepair (bp) segment of the canine papillomavirus (CPV) 16 genome located from 3295 bps (within the E2/E4 genes) to 1794 bp (located within E1 gene). A schematic showing the complete linearized CPV16 genome with gene locations is shown above the HTS assembly. The gray boxes below the HTS assembly depict the depth of coverage. The inset box on the left side of the HTS assembly highlights a viral translocation of a portion of the long control region (LCR) (blue rectangle) located at the end of the viral assembly. The inset box on the right side of the HTS assembly highlights a viral translocation of a portion of the E1 gene (red rectangle) located at the end of the viral assembly.

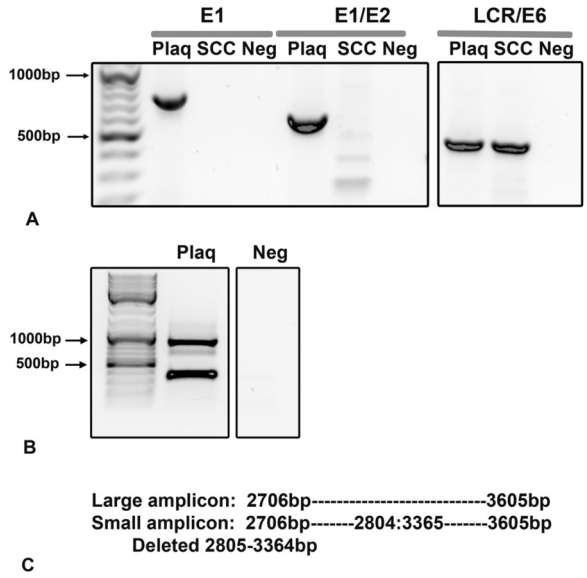

Fig. 5. (A) PCR revealed deletion of portions of the E1/E2 genes but not the long control region (LCR)/E6 gene in the sample of squamous cell carcinoma (SCC). PCR was performed using specific primers to detect a portion of the E1/E2, E1 only, and a portion of the LCR/ E6 gene of CPV16. Samples included extracted DNA from the viral plaque (Plaq) and the sample of SCC. Amplicons for the E1 and E2 genes were present only in the sample from the viral plaque but not the sample of SCC. The LCR/E6 gene was present within both samples. (B) Identification of a viral deletion within the sample from the viral plaque. PCR was performed on the sample from the viral plaque using a specific primer set that detected a portion of the E2/E4 genes. Two amplicons were generated and sequenced. (C) The large amplicon identified the expected region of the canine papillomavirus (CPV) 16 genome whereas the small amplicon contained a deletion within the CPV16 genome.

portion of the E2/E4 region of CPV16 revealed two different sized products in the plaque sample (no amplicons were generated in the SCC sample) (Fig. 5B). Sequencing of the larger amplicon identified the expected 899 bp segment spanning 2706–3605 of the CPV16 genome. Sequencing of the smaller amplicon revealed a sequence spanning from 2706 to 3605, but with a deletion of 559 bps that extended from 2805 to 3364 (Fig. 5C).

3.5. Chromosomal integration

We pursued genome walking in order to identify a potential site of integration into the host genome. Using forward primers based in the CPV16 genome, we generated a total of eight unique sequences (Table 1 and Fig. 6) by sequencing different amplicons resulting from genome walking. Two sequences spanned the CPV16 genome between 871 and 1592 and 871–1544, a segment of the E1 gene. Three other sequences identified a translocated segment of the E1 gene located at 1784 of the CPV16 sequence. Another sequence contained a portion of the E1 gene, a translocated segment of the E1 gene, followed by a sequence of canine chromosome 7. The viral breakpoint was located at 1784 bp in the CPV16 genome. One sequence contained a portion of the CPV16 E1 gene and a segment of chromosome 3 with a viral breakpoint at CPV16 1457. One final sequence contained a portion of the CPV16 E1 gene and a segment of chromosome 16, with a viral breakpoint at CPV16 1449.

Using reverse primers based in the CPV16 genome, we generated 4 unique sequences (Table 1 and Fig. 6) based upon amplicons generated from genome walking. One sequence spanned the CPV16 genome between 5218 and 5673, a segment of the L2/L1 gene. Two other unique sequences included a portion of E2/E4 gene and a translocated segment of the L1/LCR. The final sequence contained a portion of the L2 gene and a segment of chromosome 18.

The sites of integration were located upstream of the gene Piezo Type Mechanosensitive Ion Channel Component 2 (PIEZO2) and within introns of the genes Cytoplasmic Polyadenylation Element Binding Protein 1 (CPEB1), WD Repeat Domain 86 (WDR86), and Vacuolar Protein Sorting 41 (VSP41). CPEB1 is the only gene likely to play a role in cellular proliferation, but given the site of integration into an intron, it is unlikely that integration resulted in upregulation of this gene.

3.6. mRNA expression of viral gene E7

High risk HPV integration is usually considered a necessary event in the progression of cervical cancer. HPV integration results in an increased expression of the E6 and E7 viral oncogenes responsible for cell transformation. In order to determine whether the expression level of E6 and E7 were also increased in the CPV-integrated SCC lesions, quantitative PCR assays were designed specifically for CPV16 E7. The expression level of CPV16 E7 was increased by 4 folds or 13 folds within the SCC sample or metastatic SCC sample, respectively, when compared to expression within the viral plaque. It was possible that the increased level of mRNA was due to the increased copy number of the viral DNA instead of the increased activity of transcription. We measured the viral DNA copies in those lesions. Interestingly, CPV16 copy number was higher within the viral plaque sample (average 2446 copies per copy of reference gene) than either the SCC (average 68 copies per copy of reference gene) or the metastatic SCC sample (average 35 copies per copy of reference gene) (Table 2). Therefore, the level of E7 mRNA from each viral DNA was more than 150 fold higher in the SCC lesions with integrated CPV16 comparing to viral plaque with episomal ones.

4. Discussion

Viral integration and loss of viral episomes occurs routinely for the high-risk mucosal papillomavirus types present within cervical carcinomas [4]. This is not the case for human cutaneous papillomaviruses, for which there are only rare reports of viral integration and associated skin cancers are uncommon [6]. Canine papillomaviruses are similarly only rarely associated with cancer, and viral integration has never been documented for a canine papillomavirus. We have herein described an unconventional method used to sequence canine papillomavirus 16 from a canine viral plaque that progressed to squamous cell carcinoma, which led to identification of viral deletions, translocations, and four sites of viral integration.

Canine papillomavirus 16 has an organization typical of papillomaviruses, including six early genes and two late genes that encode the viral capsid. CPV16 E6 includes the typical two pairs of zinc binding motifs, which are involved in protein-protein interactions [35,40]. E7 from CPV16 contains the LXCXE peptide-binding motif, which is found in high risk HPV16, as well as other CPVs and cutaneous HPVs [41]. This motif is responsible for binding to the tumor suppressor gene retinoblastoma and inhibiting its function [37,38].

Canine papillomavirus 16 is most closely related to other canine chipapillomaviruses, with the most closely related viruses including CPV4, CPV12, and CPV9. Like all other chipapillomaviruses [22], CPV16 was identified in association with viral plaques present on the skin of a dog. However, unlike most canine viral plaques which either regress spontaneously or remain as benign lesions, the viral plaque in this dog progressed to squamous cell carcinoma and metastasized to the regional lymph nodes. There are rare reports of viral plaques progressing to squamous cell carcinoma, but even more rarely has the associated virus been identified [24,25]. Given the uncommon occurrence of a viral plaque progressing to cancer and the even more rare identification of the associated virus, it remains unknown if there are “high-risk” canine chipapillomavirus types that have a greater risk of cancer. So far, of the chipapillomaviruses, only CPV9, CPV12, and CPV16 have been associated with cancer, and each of these reported occurrences

Table 1
Identification of canine papillomavirus 16 (CPV16) genomic rearrangements and chromosomal (chr) integration sites.

Genome walking sequencing results with forward CPV16 primers	Nearby genes to chromosome integration site
CPV16 (871-1592)	
CPV16 (871-1544)	
CPV16 (871-1784) : CPV16 (1278-1425)	
CPV16 (1402-1784) : CPV16 (1278-1408)	
CPV16 (1402-1784) : CPV16 (1278-1360)	
CPV16 (1402-1784) : CPV16 (1278-1360) : Chr7 (76473226-76473372)	~4.4kb from PIEZO2
CPV16 (1402-1457) : Chr3 (54434370-54433576)	In intron of CPEB1
CPV16 (1402-1449) : Chr16 (15390857-15390266)	In intron of WDR86
Genome walking sequencing results with reverse CPV16 primers	
CPV16 (5218-5673)	
CPV16 (6651-7562) : CPV16 (3295-3343)	
CPV16 (6707-7562) : CPV16 (3295-3410)	
Chr18 (10953774-10954493) : CPV16 (4455-4717)	In intron of VPS41

PIEZO2 (Piezo Type Mechanosensitive Ion Channel Component 2); CPEB1 (Cytoplasmic Polyadenylation Element Binding Protein 1); WDR86 (WD Repeat Domain 86); VSP41 Vacuolar Protein Sorting 41.

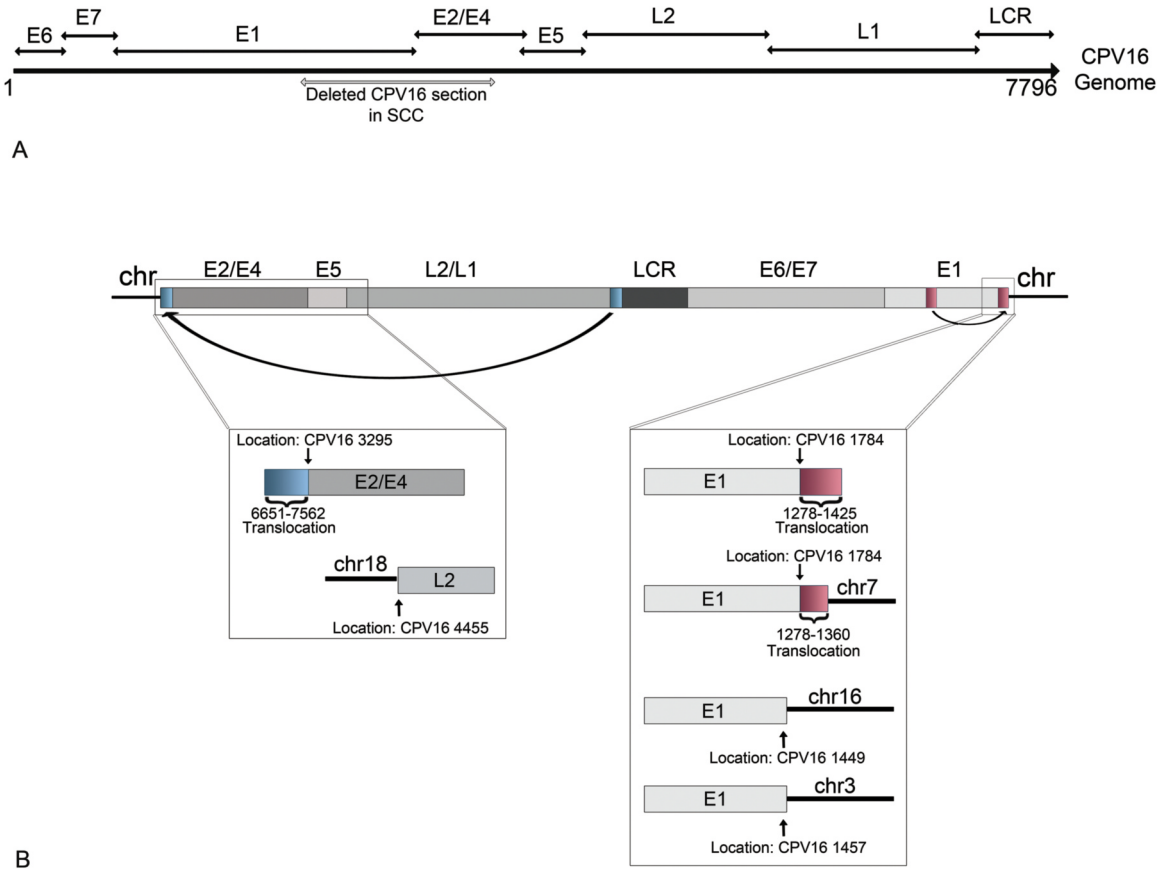

Fig. 6. Schematic representation of viral translocations and sites of viral integration into the host genome. (A) Linearized CPV16 genome including location of genes. The gray bar indicates the deleted portion of the CPV16 genome within the sample of squamous cell carcinoma (SCC). The deleted portion spans the E1 and E2/E4 genes. (B) Linearized CPV16 genome as predicated within the host genome. The inset on the left shows the results of 2 different amplicons identified with genome walking. The first includes a translocation (indicated by a blue rectangle) of a portion of the viral long control region (LCR) to the E2/E4 gene. The second identified the L2 gene integrated into canine chromosome 18. The inset on right shows 4 different amplicons identified with genome walking, including a translocation of a portion of the E1 gene (indicated by red rectangle); a translocation followed by integration into canine chromosome 7; integration of the E1 gene into chromosome 16; and integration of the E1 gene into chromosome 3.

Table 2
mRNA expression of CPV16 E7 and viral copy number within tissue samples of viral plaque and squamous cell carcinoma (SCC). CPV16 DNA copy number is expressed as copies of CPV16 DNA per copy of the reference gene RPL13A. Gene expression of CPV16 E7 is reported as a relative quantity where all samples are normalized to reference gene expression and then compared to the mean expression within the plaque sample, which is expressed as 1, to determine the fold change.

Sample	E7 mRNA expression (fold change above expression in plaque sample)	Viral copy (expressed as viral copy per copy of reference gene RPL13A)	E7 mRNA expression fold change above expression in plaque sample in control with viral copy number
Viral plaque	1	2446	1
Skin SCC	4	68	152.5
Lymph node metastatic SCC	14	35	995

CPV (canine papillomavirus virus); SCC (squamous cell carcinoma).

represents only a single dog [24,25]. Canine papillomavirus types from other genera are also rarely associated with cancer. CPV2, a taupapillomavirus, causes cutaneous papillomas that can progress to metastatic squamous cell carcinoma in a research colony of dogs with X-linked severe combined immunodeficiency [23]. CPV17, another taupapillomavirus, was the likely cause of multiple oral SCCs in a single dog and CPV1, a lambdapapillomavirus, most often causes oral papillomas but has rarely been associated with cancer [26,27,42,43]. Of all these cases of SCC, there have been no reports of viral integration into the host genome.

We demonstrated deletion of portions of the E1 and E2 genes within the SCC samples with multiple viral translocations and host integration sites. One viral translocation included a segment of the E1 gene translocated into a more distant segment of the E1 gene and a second translocation where a segment of the LCR translocated into the E2/E4 genes. We also identified 4 sites of viral integration, including 3 within the E1 gene and one within the L2 gene. As there were three viral breakpoints identified within the E1 gene, this may be a site of genetic instability within the virus. In one case, integration into chromosome 7 occurred immediately adjacent to a translocated section of E1. The other two integrations within E1 were located slightly earlier in the E1 gene; however, as these are small sequences, it is possible that these sites are located within a translocated section of E1, similar to the chromosome 7 integration site. Regardless if it was the main E1 gene or a translocated segment of E1, a portion of the E1 gene integrated into 3 different chromosomes with at least one occurring at a site of a translocation. We also identified a deletion within the viral genome in the pigmented viral plaque, suggesting that even in early lesions without overt criteria of malignancy there can be viral genomic instability.

One limitation to our study was the low and somewhat uneven coverage of the viral genome obtained with HTS. The low coverage was not entirely unexpected as the samples were from total extracted genomic DNA and most sequences aligned to the dog. It is possible that more of the genome would have been detected had we been able to get deeper coverage. We did, however, confirm loss of at least a portion of the E1 and E2 genes within the SCC using conventional PCR and have further amplified the identical translocations identified with HTS using a separate method, genome walking. Thus, while HTS may have missed portions of the viral genome, our overall findings of loss of portions of E1 and E2 and multiple translocations have been supported using other molecular methods.

The majority of human cervical cancer cases contain integrated high-risk papillomavirus, and this is widely accepted as an underlying mechanism for carcinogenesis [3,5,44,45]. The most supported hypothesis is that integration causes disruption of the E2 gene and subsequent loss of E2-mediated transcriptional repression of the E6 and E7 promoter. This loss of repression can thereby result in increased expression of E6 and E7 and ultimately unregulated cell growth [3,5,44–46]. E2 regulation can also be disrupted by methylation, with similar loss of repression of E6 and E7 expression [46]. Alternatively, integration with disruption of E1 expression could result in DNA damage and focal genomic instability [46]. In our present case, disruption of the E2 gene, and possibly E1, with loss of repression of E6 and E7 expression is the most plausible explanation in this present case. In support of this hypothesis, our results of HTS and genome walking identified sites of integration that would disrupt expression of E1 and E2. Further, E7 mRNA expression was higher within the SCC samples containing integrated forms compared with the viral plaque samples; and, this was not due simply to an increase in viral copies, as there were higher viral copies identified within the viral plaque.

In some cases of cancer, however, the HPV remains as an episome or integration occurs at a site other than E1/E2, and thus disruption and overexpression of E6 and E7 could not explain carcinogenesis in these cases [45]. Other hypotheses include viral integration within a tumor suppressor gene causing gene inactivation, viral integration flanking an oncogene resulting in overexpression, and viral integration resulting in widespread genomic instability [45,46]. None of these latter hypotheses would explain development of cancer in this present case, as integration did not occur within a tumor suppressor gene nor did it flank any oncogenes. It remains possible, however, that identification of additional integration sites may in fact support some of these alternate hypotheses. One additional hypothesis that we cannot rule out is the formation of viral—host fusion transcripts that are more stable than viral transcripts [46].

Human cutaneous papillomaviruses have been a controversial player in development of non-melanoma skin cancers in humans, but current data strongly supports a role for cutaneous papillomaviruses in the pathogenesis of non-melanoma skin cancers, particularly in immunosuppressed individuals [47–49]. These human papillomaviruses, unlike their mucosal high-risk counterparts, do not integrate into the host genome and instead remain as extrachromasomal DNA [49]. In the African multimammate mouse (*Mastomys coucha*), a preclinical model to study the effect of papillomavirus on skin carcinogenesis, natural infection with MnPV induces benign skin lesions which can transform to cancer, but the virus does not integrate into the host genome. In contrast to these other cutaneous papillomaviruses, CPV16 in this present study integrated into the host genome which likely played a role in carcinogenesis. It may be that CPV16 has a somewhat unusual behavior for cutaneous papillomaviruses and is more typical of the high-risk mucosal human papillomavirus types.

It remains to be seen if CPV16 will be an important player in development of cancer in dogs. It is likely that CPV16 was essential for carcinogenesis in this case; however, establishment of a causal association will require further demonstration of oncogene transcription within these tumors and demonstration of transforming abilities of the oncogenes. Nonetheless, this manuscript has demonstrated for the first time the ability of a cutaneous canine papillomavirus to integrate into the host genome, similar to the high-risk human papillomaviruses within cervical cancers.

5. Conclusions

Canine papillomavirus 16 was identified from a pigmented viral plaque that progressed to metastatic squamous cell carcinoma. Segments of the viral genome were deleted in the squamous cell carcinoma, including segments of the E1 and E2/E4 genes. Multiple translocations of viral genomic segments were detected within the squamous cell carcinoma sample, along with integration into four

chromosomes. This is the first report of chromosomal integration for a canine papillomavirus.

Competing interest

The authors declare that there is no conflict of interest regarding the publication of this article.

Funding

This work was supported by funds provided by the Bernice Barbour Foundation, United States and North Carolina State University's College of Veterinary Medicine, United State.

Appendix A. Supporting information

Supplementary data associated with this article can be found in the online version at doi:10.1016/j.pvr.2019.02.002.

References

[1] H.U. Bernard, R.D. Burk, Z. Chen, K. van Doorslaer, H. Hausen, E.M. de Villiers, Classification of papillomaviruses (PVs) based on 189 PV types and proposal of taxonomic amendments, Virology 401 (1) (2010) 70–79.
[2] J. Doorbar, W. Quint, L. Banks, I.G. Bravo, M. Stoler, T.R. Broker, et al., The biology and life-cycle of human papillomaviruses, Vaccine 30 (Suppl 5) (2012) F55–F70.
[3] R.P. Araldi, T.A. Sant'Ana, D.G. Modolo, T.C. de Melo, D.D. Spadacci-Morena, R. de Cassia Stocco, et al., The human papillomavirus (HPV)-related cancer biology: an overview, Biomed. Pharmacother. 106 (2018) 1537–1556.
[4] H. zur Hausen, Papillomaviruses in the causation of human cancers - a brief historical account, Virology 384 (2) (2009) 260–265.
[5] M. Kadaja, A. Sumerina, T. Verst, M. Ojarand, E. Ustav, M. Ustav, Genomic instability of the host cell induced by the human papillomavirus replication machinery, EMBO J. 26 (8) (2007) 2180–2191.
[6] K. Connolly, P. Manders, P. Earls, R.J. Epstein, Papillomavirus-associated squamous skin cancers following transplant immunosuppression: one Notch closer to control, Cancer Treat. Rev. 40 (2) (2014) 205–214.
[7] H. Delius, M.A. Van Ranst, A.B. Jenson, H. zur Hausen, J.P. Sundberg, Canine oral papillomavirus genomic sequence: a unique 1.5-kb intervening sequence between the E2 and L2 open reading frames, Virology 204 (1) (1994) 447–452.
[8] C.E. Lange, M. Ackermann, C. Favrot, K. Tobler, Entire genomic sequence of novel canine papillomavirus type 13, J. Virol. 86 (18) (2012) 10226–10227.
[9] C.E. Lange, A. Diallo, C. Zewe, L. Ferrer, Novel canine papillomavirus type 18 found in pigmented plaques, Papillomavirus Res. 2 (2016) 159–163.
[10] C.E. Lange, K. Tobler, M. Ackermann, L. Panakova, K.L. Thoday, C. Favrot, Three novel canine papillomaviruses support taxonomic clade formation, J. Gen. Virol. 90 (Pt 11) (2009) 2615–2621.
[11] C.E. Lange, K. Tobler, A. Lehner, E. Vetsch, C. Favrot, A case of a canine pigmented plaque associated with the presence of a Chi-papillomavirus, Vet. Dermatol. 23 (1) (2012) e18–e19 (76-80).
[12] C.E. Lange, K. Tobler, E.M. Schraner, E. Vetsch, N.M. Fischer, M. Ackermann, et al., Complete canine papillomavirus life cycle in pigmented lesions, Vet. Microbiol. 162 (2–4) (2013) 388–395.
[13] J. Luff, M. Mader, M. Britton, J. Fass, P. Rowland, C. Orr, et al., Complete genome sequence of canine papillomavirus type 16, Genome Announc. 3 (3) (2015).
[14] J. Luff, P. Moore, D. Zhou, J. Wang, Y. Usuda, V. Affolter, et al., Complete genome sequence of canine papillomavirus type 10, J. Virol. 86 (20) (2012) 11407.
[15] M.J. Tisza, H. Yuan, R. Schlegel, C.B. Buck, Genomic sequence of canine papillomavirus 19, Genome Announc. 4 (6) (2016).
[16] K. Tobler, C. Favrot, G. Nespeca, M. Ackermann, Detection of the prototype of a potential novel genus in the family Papillomaviridae in association with canine epidermodysplasia verruciformis, J. Gen. Virol. 87 (Pt 12) (2006) 3551–3557.
[17] K. Tobler, C. Lange, D.N. Carlotti, M. Ackermann, C. Favrot, Detection of a novel papillomavirus in pigmented plaques of four pugs, Vet. Dermatol. 19 (1) (2008) 21–25.
[18] H. Yuan, S. Ghim, J. Newsome, T. Apolinario, V. Olcese, M. Martin, et al., An epidermotropic canine papillomavirus with malignant potential contains an E5 gene and establishes a unique genus, Virology 359 (1) (2007) 28–36.
[19] H. Yuan, J. Luff, D. Zhou, J. Wang, V. Affolter, P. Moore, et al., Complete genome sequence of canine papillomavirus type 9, J. Virol. 86 (10) (2012) 5966.
[20] D. Zhou, J. Luff, S. Paul, F. Alkhilaiwi, Y. Usuda, N. Wang, et al., Complete genome sequence of canine papillomavirus virus type 12, Genome Announc. 3 (2) (2015).
[21] D. Zhou, J. Luff, Y. Usuda, V. Affolter, P. Moore, R. Schlegel, et al., Complete genome sequence of canine papillomavirus type 11, Genome Announc. 2 (3) (2014).
[22] J.S. Munday, N.A. Thomson, J.A. Luff, Papillomaviruses in dogs and cats, Vet. J. 225 (2017) 23–31.
[23] M.H. Goldschmidt, J.S. Kennedy, D.R. Kennedy, H. Yuan, D.E. Holt, M.L. Casal, et al., Severe papillomavirus infection progressing to metastatic squamous cell carcinoma in bone marrow-transplanted X-linked SCID dogs, J. Virol. 80 (13) (2006) 6621–6628.
[24] J. Luff, P. Rowland, M. Mader, C. Orr, H. Yuan, Two canine papillomaviruses associated with metastatic squamous cell carcinoma in two related Basenji dogs, Vet. Pathol. 53 (6) (2016) 1160–1163.
[25] J.S. Munday, K.I. O'Connor, B. Smits, Development of multiple pigmented viral plaques and squamous cell carcinomas in a dog infected by a novel papillomavirus, Vet. Dermatol. 22 (1) (2011) 104–110.
[26] J.S. Munday, M. Dunowska, R.E. Laurie, S. Hills, Genomic characterisation of canine papillomavirus type 17, a possible rare cause of canine oral squamous cell carcinoma, Vet. Microbiol. 182 (2016) 135–140.
[27] J.S. Munday, R.S. Tucker, M. Kiupel, C.J. Harvey, Multiple oral carcinomas associated with a novel papillomavirus in a dog, J. Vet. Diagn. Investig. 27 (2) (2015) 221–225.
[28] C.E. Lange, S. Zollinger, K. Tobler, M. Ackermann, C. Favrot, Clinically healthy skin of dogs is a potential reservoir for canine papillomaviruses, J. Clin. Microbiol. 49 (2) (2011) 707–709.
[29] H. Li, R. Durbin, Fast and accurate short read alignment with Burrows-Wheeler transform, Bioinformatics 25 (14) (2009) 1754–1760.
[30] J.G. Ruby, P. Bellare, J.L. Derisi, PRICE: software for the targeted assembly of components of (Meta) genomic sequence data, G3 3 (5) (2013) 865–880.
[31] J.A. Luff, H. Yuan, M.M. Suter, E.J. Muller, R. Schlegel, P.F. Moore, Canine keratinocytes upregulate type I interferons and proinflammatory cytokines in response to poly(dA: dt) but not to canine papillomavirus, Vet. Immunol. Immunopathol. 153 (3–4) (2013) 177–186.
[32] K.J. Livak, T.D. Schmittgen, Analysis of relative gene expression data using real-time quantitative PCR and the 2(-Delta Delta C(T)) Method, Methods 25 (4) (2001) 402–408.
[33] E.M. de Villiers, C. Fauquet, T.R. Broker, H.U. Bernard, H. zur Hausen, Classification of papillomaviruses, Virology 324 (1) (2004) 17–27.
[34] E.M. de Villiers, C. Whitley, K. Gunst, Identification of new papillomavirus types, Methods Mol. Med. 119 (2005) 1–13.
[35] M.S. Barbosa, D.R. Lowy, J.T. Schiller, Papillomavirus polypeptides E6 and E7 are zinc-binding proteins, J. Virol. 63 (3) (1989) 1404–1407.
[36] A.M. Helt, D.A. Galloway, Destabilization of the retinoblastoma tumor suppressor by human papillomavirus type 16 E7 is not sufficient to overcome cell cycle arrest in human keratinocytes, J. Virol. 75 (15) (2001) 6737–6747.
[37] X. Liu, A. Clements, K. Zhao, R. Marmorstein, Structure of the human papillomavirus E7 oncoprotein and its mechanism for inactivation of the retinoblastoma tumor suppressor, J. Biol. Chem. 281 (1) (2006) 578–586.
[38] K. Munger, B.A. Werness, N. Dyson, W.C. Phelps, E. Harlow, P.M. Howley, Complex formation of human papillomavirus E7 proteins with the retinoblastoma tumor suppressor gene product, EMBO J. 8 (13) (1989) 4099–4105.
[39] J. Wang, D. Zhou, A. Prabhu, R. Schlegel, H. Yuan, The canine papillomavirus and gamma HPV E7 proteins use an alternative domain to bind and destabilize the retinoblastoma protein, PLoS Pathog. 6 (9) (2010) e1001089.
[40] M. Lagrange, S. Charbonnier, G. Orfanoudakis, P. Robinson, K. Zanier, M. Masson, et al., Binding of human papillomavirus 16 E6 to p53 and E6AP is impaired by monoclonal antibodies directed against the second zinc-binding domain of E6, J. Gen. Virol. 86 (Pt 4) (2005) 1001–1007.
[41] A. Dahiya, M.R. Gavin, R.X. Luo, D.C. Dean, Role of the LXCXE binding site in Rb function, Mol. Cell Biol. 20 (18) (2000) 6799–6805.
[42] C.L. Bregman, R.S. Hirth, J.P. Sundberg, E.F. Christensen, Cutaneous neoplasms in dogs associated with canine oral papillomavirus vaccine, Vet. Pathol. 24 (6) (1987) 477–487.
[43] A.M. Regalado Ibarra, L. Legendre, J.S. Munday, Malignant transformation of a canine papillomavirus type 1-induced persistent oral papilloma in a 3-year-old dog, J. Vet. Dent. 35 (2) (2018) 79–95.
[44] M. Kadaja, T. Silla, E. Ustav, M. Ustav, Papillomavirus DNA replication - from initiation to genomic instability, Virology 384 (2) (2009) 360–368.
[45] M.A. Oyervides-Munoz, A.A. Perez-Maya, H.F. Rodriguez-Gutierrez, G.S. Gomez-Macias, O.R. Fajardo-Ramirez, V. Trevino, et al., Understanding the HPV integration and its progression to cervical cancer, Infect. Genet. Evol. 61 (2018) 134–144.
[46] A.A. McBride, A. Warburton, The role of integration in oncogenic progression of HPV-associated cancers, PLoS Pathog. 13 (4) (2017) e1006211.
[47] J.W. Leiding, S.M. Holland, Warts and all: human papillomavirus in primary immunodeficiencies, J. Allergy Clin. Immunol. 130 (5) (2012) 1030–1048.
[48] N.M. Reusser, C. Downing, J. Guidry, S.K. Tyring, HPV carcinomas in immunocompromised patients, J. Clin. Med. 4 (2) (2015) 260–281.
[49] D. Hasche, S.E. Vinzon, F. Rosl, Cutaneous papillomaviruses and non-melanoma skin cancer: causal agents or innocent bystanders? Front. Microbiol. 9 (2018) 874.